



HAL
open science

Nonlinear Ultrasonic Waves for Structural Health Monitoring

Claudio Nucera, Francesco Lanza Di Scalea

► **To cite this version:**

Claudio Nucera, Francesco Lanza Di Scalea. Nonlinear Ultrasonic Waves for Structural Health Monitoring. EWSHM - 7th European Workshop on Structural Health Monitoring, IFSTTAR, Inria, Université de Nantes, Jul 2014, Nantes, France. hal-01021068

HAL Id: hal-01021068

<https://inria.hal.science/hal-01021068>

Submitted on 9 Jul 2014

HAL is a multi-disciplinary open access archive for the deposit and dissemination of scientific research documents, whether they are published or not. The documents may come from teaching and research institutions in France or abroad, or from public or private research centers.

L'archive ouverte pluridisciplinaire **HAL**, est destinée au dépôt et à la diffusion de documents scientifiques de niveau recherche, publiés ou non, émanant des établissements d'enseignement et de recherche français ou étrangers, des laboratoires publics ou privés.

NONLINEAR ULTRASONIC WAVES FOR STRUCTURAL HEALTH MONITORING

Claudio Nucera and Francesco Lanza di Scalea

University of California, San Diego, Department of Structural Engineering, 9500 Gilman Drive,
M.C. 0085, La Jolla, California, 92093-0085 USA

cnucera@ucsd.edu

ABSTRACT

Nonlinear ultrasonic waves in solids have shown good sensitivity to quasi-static stresses. The stress sensitivity of elastic waves is typically associated to finite strains (e.g. theory of acoustoelasticity). In the case of waveguides, classical nonlinear theories for guided waves are still based on the assumption of finite strains. In the case of constrained solids subjected to thermal excursions, however, there are theoretically no finite strains (for perfectly-constrained solids) associated with thermal stresses. A new model is therefore needed to justify the existence of wave nonlinearities in this case of stress without strain. This problem is solved on the basis of the interatomic potential of the solid that indicates a “residual” strain energy, due to the prevented thermal expansion, that is at least cubic as a function of strain. The cubic relationship between strain energy and strain produces second-harmonic generation of propagating elastic waves. Consequently, a nonlinear wave equation can be derived. The solution to this equation leads to a new nonlinear parameter for double harmonic generation that is directly related to the thermal stresses in the structure. The present study finds applications in the monitoring of thermal stresses in buckling-prone structures, such as continuously-welded railroad tracks and pipelines.

KEYWORDS : *Nonlinear Guided Waves, Higher-Harmonics, Interatomic Potential, Constrained Thermal Expansion.*

1 INTRODUCTION

Different mechanisms can give rise to nonlinear effects in elastic wave propagation within nonlinear solids. First, the amplitude of the elastic wave may be sufficiently large so that finite deformations arise. Second, a material which behaves in a linear manner when undeformed may respond nonlinearly when infinitesimal ultrasonic waves are propagated, provided that a sufficient amount of external static stress is superimposed. In a third instance, the material itself may exhibit various energy absorbing mechanisms or particular forms of strain energy potentials that, under specific boundary conditions and external excitations, lead to a nonlinear response. This is the case of a constrained thermal expansion of a solid that develops thermal stresses without quasi-static strains.

Higher-harmonic generation is one of the possible manifestations of nonlinearity and is considered in this paper. According to this phenomenon, a sinusoidal stress wave of a given frequency distorts as it propagates through the nonlinear waveguide, and energy is transferred from the fundamental frequency, ω , to the higher harmonics, 2ω , 3ω , and so on. This particular effect has been exploited in recent years to detect macroscopic cracks [1], material degradation [2], fatigue damage in metallic structures [3, 4], bonding defects in adhesive joints [5], thermal fatigue in composites [6], and damage in concrete structures [7].

A much less investigated application of nonlinearity-driven higher-harmonic generation is the measurement of quasi-static stresses/loads in structures. In this area an attractive application is the measurement of thermal stresses arising from constrained thermal expansions of solids in order to prevent thermal buckling of structures. A specific case of interest is the management of the thermal

stresses arising in Continuous-Welded Rail (CWR) during temperature excursion [8, 9]. Generally, these thermal stresses are unknown, and they are the cause of several accidents worldwide. According to U.S. Safety Statistics data [10] in 2010 irregular track alignment from buckling or sunkink was the first cause of train accidents in the U.S. within the categories of track, roadbed and structures, responsible for the highest cost of \$17M or 15% of the total damage cost from these categories. A system that is able to determine the level of thermal stress in a rail track, or even just the temperature at which the thermal stresses are zero (known as the rail “Neutral Temperature”), has long been desired by the railroad industry. The proposed model could be very beneficial for this case.

2 PROPOSED NONLINER WAVEGUIDE MODEL

Nonlinear phenomena arising in wave propagation have been classically treated using acoustoelasticity [11] or Finite Amplitude Wave theory [12]. According to these frameworks, applied finite strains (or, similarly, finite amplitude waves) constitute a requirement for the occurrence of nonlinearity. However, the generation of nonlinear effects in solids (higher harmonics in particular) subjected to constrained thermal expansion requires a different theoretical perspective. When the constrained structure experiences temperature changes, it cannot globally deform because of the boundaries while, at the same time, the lattice particles acquire an increased energy of vibration (proportional to temperature) in agreement with classical material science theories [13]. The absence of quasi-static strains makes this case different from classical sources of nonlinear wave propagation.

2.1 Interatomic Potential

The concept of interatomic potential allows to find the relationship between elastic potential energy and deformations at the atomistic level. The general form for the interatomic potential of a solid for a pair of lattice particles can be written as [14]:

$$V_{MIE}(r) = \left(\frac{n}{n-m}\right) \left(\frac{n}{m}\right)^{\frac{m}{n-m}} w \left[\left(\frac{q}{r}\right)^n - \left(\frac{q}{r}\right)^m \right] \quad (1)$$

where r is the Interatomic Distance, w is the Potential Well Depth, q is the Van Der Waals Radius, n and m are material coefficient parameters. The interatomic force is given by the first derivative of the potential, therefore:

$$F_{MIE}(r) = -\frac{dV_{MIE}}{dr} = -\frac{n \left(\frac{n}{m}\right)^{\frac{m}{n-m}} w \left[m \left(\frac{q}{r}\right)^m - n \left(\frac{q}{r}\right)^n \right]}{r(n-m)} \quad (2)$$

Eq. (2) contains a steep “repulsive” part (first term in the square brackets), and a smoother “attractive” part (second term in the square brackets). The minimum of the $V(r)$ curve is the position of equilibrium of the atoms, r_0 , where the repulsive force is equilibrated by the attractive force and the net force is zero. A specific form of the interatomic potential most often used for its computational efficiency was proposed by Lennard-Jones [15-17], where $n = 12$ and $m = 6$. From Eq. (1), the Lennard-Jones potential is therefore:

$$V_{LJ} = 4w \left[\left(\frac{q}{r}\right)^{12} - \left(\frac{q}{r}\right)^6 \right] \quad (3)$$

2.2 Potential Energy for Constrained Thermal Expansion

Assuming that the solid is free to expand, an increase in temperature produces a stretch of the atoms’ equilibrium distance r_0 , following the dashed curve in Fig. 1. This curve is the so-called *Average Bonding Distance* (ABD), or the loci of midpoints between repulsive and attractive branches of the potential. The ABD curve represents the well-known thermal expansion of the

material, which directly results from the “anharmonicity” of the interatomic potential curve. The analytical form of the ABD curve, $r_{ABD}(V)$, can be easily obtained from a general Mie potential with $n = 2m$ by equating the repulsive force to the attractive force:

$$r_{ABD} = 2^{\left(\frac{1}{m}-1\right)} q \left[\left(1 - \sqrt{1 + \frac{V}{w}}\right)^{-\frac{1}{m}} + \left(1 + \sqrt{1 + \frac{V}{w}}\right)^{-\frac{1}{m}} \right] \quad (4)$$

Following conventional linearized thermal expansion theory, the r_{ABD} curve can be also simply written as a function of temperature as:

$$r_{ABD}(T) = r_0 [1 + \alpha(T - T_0)] \quad (5)$$

where α is the thermal expansion coefficient of the material, and $\Delta T = T - T_0$ is the temperature change from the initial interatomic distance r_0 . For free thermal expansion, the minima of the interatomic potential curve at the various temperatures lie on the r_{ABD} curve, and the Potential Well depth rises to reflect the additional kinetic energy imparted by the temperature increase. In this case, the new positions of the atoms at all temperatures are still at zero net force (strain without stress). If, instead, the solid is prevented from thermally expanding due to external constraints, it is known that it develops thermal stresses. This fact, in turn, implies that the interatomic potential at T does not have a minimum point (zero force), but it assumes a value that corresponds to the $V(r)$ curve for the original T_0 temperature, calculated at the current “free expansion” position $r_{ABD}(T)$ (see Fig. 1).

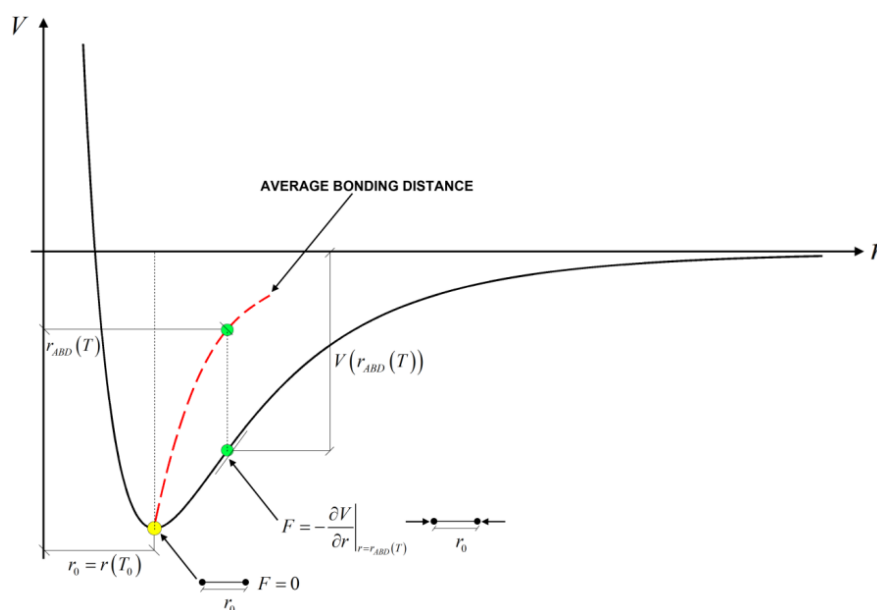


Fig. 1 – ABD curve for free expansion and residual potential for perfectly-constrained thermal expansion.

For such case of constrained thermal expansion, the general form of the current interatomic potential at T can be found by expanding Eq. (1) around the $r_{ABD}(T)$ value. The result is:

$$\begin{aligned} V(r, T) &= V(r_{ABD}(T)) + \left. \frac{\partial V}{\partial r} \right|_{r=r_{ABD}(T)} \cdot (r - r_{ABD}(T)) + \frac{1}{2} \left. \frac{\partial^2 V}{\partial r^2} \right|_{r=r_{ABD}(T)} \cdot (r - r_{ABD}(T))^2 + \\ &+ \frac{1}{6} \left. \frac{\partial^3 V}{\partial r^3} \right|_{r=r_{ABD}(T)} \cdot (r - r_{ABD}(T))^3 + \dots = \\ &= A(T) + B(T) \cdot (r - r_{ABD}(T)) + \frac{1}{2} C(T) \cdot (r - r_{ABD}(T))^2 + \frac{1}{6} D(T) \cdot (r - r_{ABD}(T))^3 + \dots \end{aligned} \quad (6)$$

where $A(T)$ is an initial energy, $B(T) = \partial V / \partial r$, $C(T) = \partial^2 V / \partial r^2$, and $D(T) = \partial^3 V / \partial r^3$, with the derivatives calculated at $r = r_{ABD}(T)$. The Taylor expansion is limited the cubic order $O(r^3)$ since the

interest in this work is the study of second-harmonic wave generation (the expansion could be easily extended further to study higher-order harmonics generation). The terms $C(T)$ and $D(T)$ in the above equation are analogous to the elastic constants of classical nonlinear elasticity caused by finite quasi-static deformations or finite-amplitude waves [18]. For example, the term C is equivalent to the second-order elastic stiffness, and the term D is equivalent to the third-order elastic stiffness. The difference with classical finite-deformation nonlinear elasticity, however, is that the nonlinearity (arising from the $O(r^3)$ term in the potential, or the term D), in this case does not arise from applied finite deformations (these are ideally zero for perfectly constrained thermal expansion), but rather from the “residual” strain energy stored as internal forces from the prevented thermal expansion.

2.3 Nonlinear Wave Equation for Constrained Thermal Expansion

Classical equilibrium considerations lead to the derivation of the nonlinear wave equation for the case under investigation. Extending Eq. (6) to a 1-D lattice comprising p particles, and assuming an infinitesimal deformation of the system Δu from an initial equilibrium state, the overall elastic potential of the p particles can be expressed as:

$$V = A(T) + \sum_p B(T) \cdot \Delta u + \frac{1}{2} \sum_p C(T) \cdot \Delta u^2 + \frac{1}{6} \sum_p D(T) \cdot \Delta u^3 + \dots \quad (7)$$

Applying Newton’s second law to the n th particle, the differential equation governing its motion reads:

$$m \frac{d^2 u_n}{dt^2} = C(T) \cdot [(u_{n+1} - u_n) - (u_n - u_{n-1})] + \frac{1}{2} D(T) \cdot [(u_{n+1} - u_n)^2 - (u_n - u_{n-1})^2] + \dots \quad (8)$$

Eq. (8) can be reformulated in order to highlight the force exerted on the generic n th particle by adjacent particles $n+1$ and $n-1$:

$$m \frac{d^2 u_n}{dt^2} = F_{n,n+1} - F_{n,n-1} = \left[B(T) + C(T) \cdot \left(\frac{u_{n+1} - u_n}{h} \right) h + \frac{1}{2} D(T) \cdot \left(\frac{u_{n+1} - u_n}{h} \right)^2 h^2 \right] - \left[B(T) + C(T) \cdot \left(\frac{u_n - u_{n-1}}{h} \right) h + \frac{1}{2} D(T) \cdot \left(\frac{u_n - u_{n-1}}{h} \right)^2 h^2 \right] + \dots \quad (9)$$

where the term h indicates the original undeformed distance between adjacent particles.

The extension to the 3D case simply follows transferring all the concepts applied for the n th particle to the n th plane. In order to simplify the treatment without any loss in generality, the resulting equation of motion will be derived for the case of 1D longitudinal bulk waves propagating along direction x_1 . Introducing the unit surface S_1 , perpendicular to axis x_1 , the equation of motion for the n th plane becomes:

$$\frac{m}{S_1} \frac{d^2 u_{1,n}}{dt^2} = \frac{F_{n,n+1}}{S_1} - \frac{F_{n,n-1}}{S_1} = \frac{C(T)h_1}{S_1} \left[\left(\frac{u_{1,n+1} - u_{1,n}}{h_1} \right) - \left(\frac{u_{1,n} - u_{1,n-1}}{h_1} \right) \right] + \frac{1}{2} \frac{D(T)h_1^2}{S_1} \left[\left(\frac{u_{1,n+1} - u_{1,n}}{h_1} \right)^2 - \left(\frac{u_{1,n} - u_{1,n-1}}{h_1} \right)^2 \right] + \dots \quad (10)$$

where the term h_1 indicates the original undeformed distance along direction x_1 between adjacent particles. The transition from the discrete system to its continuum counterpart is simply accomplished letting the term h_1 tend to zero in Eq. (10). Exploiting the definition of derivative, in the continuum limit Eq. (10) can be rearranged as:

$$\frac{m}{S_1} \frac{d^2 u_{1,n}}{dt^2} = \frac{F_1(x_1)}{S_1} - \frac{F_1(x_1 - h_1)}{S_1} = \sigma_{11}(x_1) - \sigma_{11}(x_1 - h_1) = \frac{C(T)h_1}{S_1} \left[\left(\frac{\partial u_1}{\partial x_1} \right)_{x_1} - \left(\frac{\partial u_1}{\partial x_1} \right)_{x_1 - h_1} \right] + \frac{1}{2} \frac{D(T)h_1^2}{S_1} \left[\left(\frac{\partial u_1}{\partial x_1} \right)_{x_1}^2 - \left(\frac{\partial u_1}{\partial x_1} \right)_{x_1 - h_1}^2 \right] + \dots \quad (11)$$

By dividing Eq. (11) by h_1 , letting h_1 tend to zero for the continuum limit, and letting $m/(S_1 h_1) = \rho$ (the mass density of the material in the initial configuration), one can derive:

$$\frac{\partial^2 u_1}{\partial t^2} = \bar{V}_1^2 \left[1 - \bar{\gamma}_1 \left(\frac{\partial u_1}{\partial x_1} \right) \right] \frac{\partial^2 u_1}{\partial x_1^2} \tag{12}$$

where the new temperature-dependent elastic coefficients of second-order and third-order are: $\bar{C}_2 = C(T)h_1 / S_1$ and $\bar{C}_3 = D(T)h_1^2 / S_1$. The terms \bar{C}_2 and \bar{C}_3 combine the influence of the classical elastic potential with the new nonlinear effects caused by the prevented thermal expansion.

The result in Eq. (12) represents the nonlinear partial differential equation governing the propagation of longitudinal bulk waves for solids subjected to constrained thermal expansion. In light of the above result, the two new definitions for longitudinal bulk wave velocity and nonlinear parameter are:

$$\bar{V}_1 = \sqrt{\frac{\bar{C}_2}{\rho}} = \sqrt{\frac{C(T)h_1}{\rho S_1}} \quad \text{LONGITUDINAL WAVE SPEED} \tag{13}$$

$$\bar{\gamma}_1 = -\frac{\bar{C}_3}{\bar{C}_2} = -\frac{D(T)h_1}{C(T)} \quad \text{NONLINEAR PARAMETER} \tag{14}$$

A dimensional analysis confirms the nature of these parameters. Since, from Eq. (7), $C(T)$ has units of *Joule/m²*, and $D(T)$ has units of *Joule/m³*, Eqs. (13) and (14) indicate that \bar{V}_1 has units of velocity (*m/sec*), and $\bar{\gamma}_1$ is dimensionless.

As expected, Eq. (13) shows that the wave speed depends on the quadratic term $O(r^2)$ of the interatomic potential, $C(T)$. This term reflects the curvature of the interatomic potential, which is changing with interatomic distance. In classical linear Hooke's theory, this curvature (hence material stiffness) is approximated constant through the deformation range, hence the wave velocity is a constant. By considering the full asymmetric potential as a function of the prevented thermal expansion, the wave velocity is found to change with accumulating thermal stresses. Trends of \bar{V}_1 from Eq. (13) are plotted in Fig. 2 assuming a Lennard-Jones interatomic potential ($n = 12, n = 6$) and sample values of Van Der Waals Radius $q = 4$ Angstroms, and Potential Well Depth $w = 40$ kJ/mol, without loss of generality for the trends. The material density is assumed that of steel, $\rho = 7800$ kg/m³.

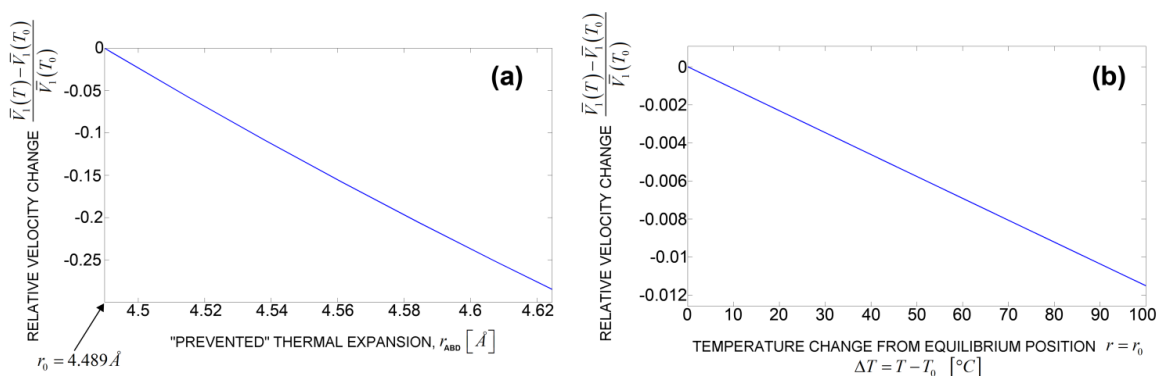


Fig. 2 - Relative change in longitudinal wave velocity as a function of: (a) “prevented” thermal expansion of interatomic distance, and (b) temperature change from stress-free position (Lennard-Jones potential, $n = 12, n = 6, q = 4$ Angstroms, $w = 40$ kJ/mol, $\alpha = 11 \times 10^{-6}/^\circ\text{C}$, $\rho = 7800$ kg/m³).

Specifically, Fig. 2a plots the relative change in wave speed, as a function of interatomic distance r_{ABD} . The temperature T_0 is the stress-free value (corresponding to equilibrium distance $r_0 = 4.489$ Angstroms - minimum of the assumed Lennard-Jones potential). The trend in Fig. 2a clearly indicates a decrease in wave speed with increasing (prevented) thermal expansion. Therefore

a material “softening” effect takes place, consistently with the decrease in curvature of the interatomic potential, $C(T)$, when moving slightly to the right of the equilibrium position r_0 (see, for example, Fig. 1). Fig. 2b plots the same velocity change as a direct function of the temperature change, $\Delta T = T - T_0$. This plot was obtained from the previous values in Fig. 2a by simply using the linear thermal expansion relation in Eq. (5), and assuming a thermal expansion coefficient for steel of $\alpha = 11 \times 10^{-6}/^\circ\text{C}$. The range of temperature excursion considered in Fig. 2b was arbitrarily chosen as 100 °C. For the case considered, for example, the longitudinal wave velocity is expected to decrease by about 1% for a temperature increase of 100°C in the fully-constrained solid.

Regarding the nonlinear parameter of Eq. (14), it contains the nonlinear portion of the interatomic potential through the cubic term $O(r^3)$, $D(T)$. Again, the difference from classical nonlinear wave theory is that the cubic $O(r^3)$ energy term arises from the prevented thermal expansion due to the asymmetry of the interatomic potential, rather than from applied finite deformations. The nonlinear parameter is discussed more in depth in the next Section.

2.4 Solution of the Nonlinear Wave Equation : Second-Harmonic Wave Generation for Constrained Thermal Expansion

Eq. (12) can be solved by using perturbation analysis [12], thereby decomposing the displacement field into the linear portion, $u_1^{(1)}$, and the nonlinear portion, $u_1^{(2)}$, with $u_1^{(1)} \ll u_1^{(2)}$.

The final solution to the nonlinear wave equation can be written in the classical form as:

$$u_1 = u_1^{(1)} + u_1^{(2)} = A_1 \cos(kx_1 - \omega t) - \frac{1}{8} \overline{\gamma}_1 k^2 A_1^2 x_1 \sin 2(kx_1 - \omega t) \quad (15)$$

where x_1 is the wave propagation distance, and k is the wavenumber.

It can be seen that the nonlinearity generates a second-harmonic contribution at 2ω under a fundamental excitation at ω . The magnitude of the second-harmonic is proportional to the nonlinear parameter given in Eq. (14), and also proportional to the wave propagation distance, x_1 (“cumulative” behavior). As in classical nonlinear wave theory, Eq. (15) only holds for a limited propagation distance that satisfies the perturbation condition $u_1^{(1)} \ll u_1^{(2)}$.

Experimentally, it is common to directly measure the amplitudes of the second-harmonic, A_2 , and that of the fundamental frequency, A_1 . Therefore, an “experimental” nonlinear parameter can be defined from the “theoretical” nonlinear parameter in Eq. (14) as:

$$\beta = \frac{|A_2|}{A_1^2} = \frac{1}{8} \overline{\gamma}_1 k^2 x_1 = \frac{\pi^2}{2} \overline{\gamma}_1 \frac{f^2}{V_1^2} x_1 \quad \text{EXPER. NONLINEAR PARAMETER (16)}$$

where f is the excitation wave frequency (fundamental), \overline{V}_1 is the longitudinal bulk wave speed, and x_1 is the wave propagation distance. Substituting Eqs. (13) and (14) into Eq. (16), the experimental nonlinear parameter can be also written in terms of the second-order and third-order energy terms, $C(T)$ and $D(T)$, as:

$$\beta(T) = \frac{|A_2|}{A_1^2} = -\frac{D(T)}{C^2(T)} \frac{\pi^2 \rho S_1 x_1 f^2}{2} \quad \text{EXPER. NONLINEAR PARAMETER (17)}$$

where $C(T) = \partial^2 V / \partial r^2$, $D(T) = \partial^3 V / \partial r^3$, and the derivatives are calculated at $r = r_{ABD}(T)$

Trends of the nonlinear parameter β from Eq. (17) are plotted in Fig. 3 assuming a Lennard-Jones interatomic potential ($n = 12$, $n = 6$) and sample values of $q = 4$ Angstroms, and $w = 40$ kJ/mol, without loss of generality for the nonlinear trends. The β values in this figure have been normalized to all terms independent of temperature, to highlight the effect of the temperature-dependent terms $C(T)$ and $D(T)$.

Fig. 3a plots β as a function of interatomic distance r_{ABD} . The nonlinear parameter increases monotonically with increasing “prevented” thermal expansion, i.e. increasing thermal stress

absorbed by the constrained solid. This trend is the combined effect of a decreasing curvature of the interatomic potential, $C(T)$ (that is also responsible for the wave velocity decrease discussed in the previous Section), and an increasing cubic term $D(T)$. Fig. 3b plots the same nonlinear parameter β as a direct function of the temperature change, $\Delta T = T - T_0$, from the initial, stress-free temperature T_0 (corresponding to equilibrium distance r_0). This plot was obtained directly from the previous values in Fig. 3a by simply using the linear thermal expansion relation Eq. (5) and assuming, again, $\alpha = 11 \cdot 10^{-6}/^\circ\text{C}$ (steel) and a fully-constrained case. The range of temperature excursion considered in Fig. 3b was arbitrarily chosen as 100 °C. It is clear that the nonlinear parameter monotonically increases with increasing temperature, as the constrained thermal expansion builds nonlinear effects through thermal stresses. The slope of the $\langle \beta \text{ vs. } T \rangle$ curve will, of course, depend on the coefficient of thermal expansion of the material, with larger slopes expected for larger α 's.

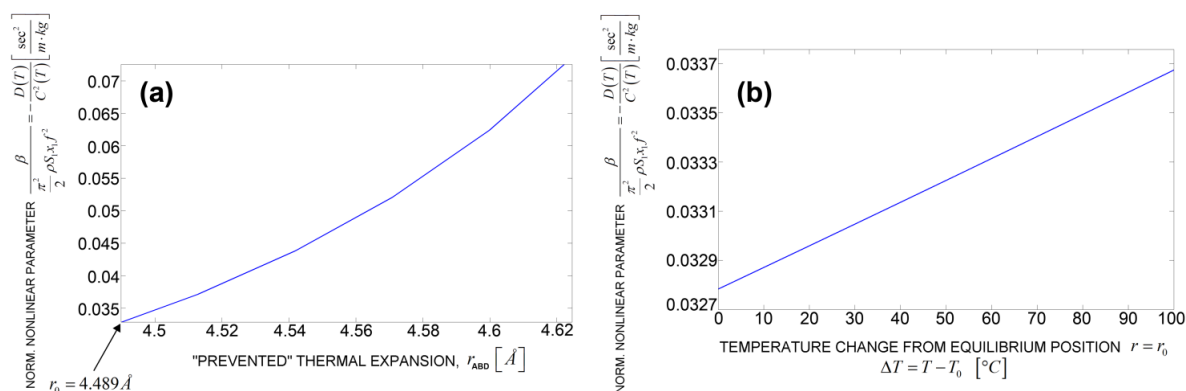


Fig. 3 - Normalized nonlinear parameter β as a function of: (a) “prevented” thermal expansion of interatomic distance, and (b) temperature change from stress-free position (Lennard-Jones potential, $n = 12$, $n = 6$, $q = 4$ Angstroms, $w = 40$ kJ/mol, $\alpha = 11 \times 10^{-6}/^\circ\text{C}$).

CONCLUSION

This work has investigated the generation of nonlinearities in ultrasonic longitudinal bulk waves propagating in constrained solids subjected to temperature increase. One potential application of this research is the possibility to detect thermal stresses caused by constrained thermal expansion in continuous-welded rail tracks and in other structures that are prone to buckling failures at high temperatures (pipes). In contrast with the classical treatment of nonlinearity in elastic wave propagation (e.g. acoustoelasticity), the present work theoretically explains nonlinear effects via the anharmonicity of the interatomic potential and the “residual” energy that is stored in the solid when it is prevented from expanding. These considerations result in an interatomic potential expression that is at least cubic, $O(r^3)$, as a function of interatomic distance. This leads to a nonlinear wave equation that can be readily solved using perturbation techniques.

Closed-form solutions for the longitudinal wave velocity and second-harmonic nonlinear parameter are presented. They are explicitly dependent on the interatomic potential parameters and on temperature. The theoretical results indicate that the longitudinal wave speed decreases with increasing temperature for a constrained solid, as a result of the resulting thermal stresses. In addition, the theory concludes that the second-harmonic nonlinear parameter increases with increasing temperature for the constrained solid.

This study suggests the potential of measuring the absolute values of thermal stresses from prevented thermal expansion by tracking the ultrasonic nonlinear parameter. However, careful calibration of all material properties involved in Eq. (17) would be required in this case. Furthermore, as in any nonlinear ultrasonic test, the nonlinearity of the instrumentation and that of the transducer/structure coupling will affect the absolute measurements. However, what would be certainly easier to determine is the point of *zero thermal stress* under a temperature fluctuation that

corresponds to a minimum of the nonlinear parameter. For example, the zero thermal stress point is a key factor in the maintenance of continuous-welded rail tracks (the well-known “neutral temperature” point of rails). The model developed is limited to longitudinal bulk waves and does not include wave attenuation/damping effects. The extension of this study to other wave modes, including dispersive guided waves propagating in prismatic structures, is underway.

ACKNOWLEDGEMENTS

This work was primarily supported by the U.S. Federal Railroad Administration grant FR-RRD-0009-10-01-03. Mahmood Fateh (Program Manager), Leith Al-Nazer and Gary Carr of the FRA provided important technical support and advice throughout the project. Partial support was also provided by the National Science Foundation grant #1028365 with George Maracas as the Program Manager.

REFERENCES

- [1] Z. Parsons, and W. J. Staszewski, “Nonlinear acoustics with low-profile piezoceramic excitation for crack detection in metallic structures,” *Smart Materials & Structures*, 15(4), 1110-1118 (2006).
- [2] H. Jeong, S. H. Nahm, K. Y. Jhang *et al.*, “Evaluation of fracture toughness degradation of CrMoV rotor steels based on ultrasonic nonlinearity measurements,” *Ksme International Journal*, 16(2), 147-154 (2002).
- [3] J. H. Cantrell, “Quantitative assessment of fatigue damage accumulation in wavy slip metals from acoustic harmonic generation,” *Philosophical Magazine*, 86(11), 1539-1554 (2006).
- [4] W. T. Yost, and J. H. Cantrell, “The effects of fatigue on acoustic nonlinearity in aluminum alloys,” *Proc. IEEE* 2, 947-955 (1992).
- [5] D. W. Yan, S. A. Neild, and B. W. Drinkwater, “Modelling and measurement of the nonlinear behaviour of kissing bonds in adhesive joints,” *NDT&E International*, 47, 18-25 (2012).
- [6] W. Li, Y. Cho, and J. D. Achenbach, “Detection of thermal fatigue in composites by second harmonic Lamb waves,” *Smart Materials and Structures*, 21(8), 1-8 (2012).
- [7] A. A. Shah, and Y. Ribakov, “Non-linear ultrasonic evaluation of damaged concrete based on higher order harmonic generation,” *Materials & Design*, 30(10), 4095-4102 (2009).
- [8] A. D. Kerr, “Thermal Buckling of Straight Tracks: Fundamentals, Analyses and Preventive Measures,” Technical Report FRA/ORD-78-49, (1978).
- [9] C. Nucera, R. Phillips, F. Lanza di Scalea *et al.*, “RAIL-NT System for the In-situ Measurement of Neutral Temperature in CWR: Results from Laboratory and Field Test,” *Journal of the Transportation Research Board*, (2013).
- [10] Federal-Railroad-Administration, [FRA Safety Statistics Data], (2011).
- [11] D. M. Egle, and D. E. Bray, “Measurement of Acoustoelastic and 3rd-Order Elastic-Constants for Rail Steel,” *Journal of the Acoustical Society of America*, 60(3), 741-744 (1976).
- [12] W. J. N. de Lima, and M. F. Hamilton, “Finite-amplitude waves in isotropic elastic plates,” *Journal of Sound and Vibration*, 265(4), 819-839 (2003).
- [13] R. J. D. Tilley, [Understanding solids : the science of materials] J. Wiley, Chichester, West Sussex, England ; Hoboken, NJ, USA(2004).
- [14] G. Mie, “Zur kinetischen Theorie der einatomigen Körper,” *Annalen Der Physik*, 316(8), 657-697 (1903).
- [15] J. E. Lennard-Jones, “On the determination of molecular fields III - From crystal measurements and kinetic theory data,” *Proceedings of the Royal Society of London Series a-Containing Papers of a Mathematical and Physical Character*, 106(740), 709-718 (1924).
- [16] J. E. Lennard-Jones, “On the determination of molecular fields II - From the equation of state of a gas,” *Proceedings of the Royal Society of London Series a-Containing Papers of a Mathematical and Physical Character*, 106(738), 463-477 (1924).
- [17] J. E. Lennard-Jones, “On the determination of molecular fields I - From the variation of the viscosity of a gas with temperature,” *Proceedings of the Royal Society of London. Series A*, 106(738), 441-462 (1924).
- [18] J. H. Cantrell, [Fundamentals and Applications of Nonlinear Ultrasonic Nondestructive Evaluation] CRC Press, Boca Raton, FL, 6 (2004).